Supplementary material

"Identification of nanocrystalline goethite in reduced clay formations. Application to the Callovian-Oxfordian formation of Bure (France)"

by

Myriam Kars, Catherine Lerouge, Sylvain Grangeon, Charles Aubourg, Christophe Tournassat, Benoît Madé and Francis Claret

1. Study on Fe-bearing samples

1.1 Samples selection

A set of Fe-bearing samples were also studied in order to determine their magnetic behavior and contribution in the bulk magnetic signature of the COx claystones.

Pure iron-bearing minerals separates were selected and their magnetic behavior under low temperature was recorded. A particular attention was brought to Fe(III) bearing minerals. The samples listed in the Table A1 are briefly described below.

Clay minerals and micas are paramagnetic at room temperature, but some of them could present magnetic ordering at very low temperature (Coey et al., 1981; Ballet and Coey, 1982; Martín-Hernández and Hirt, 2003; Rivas-Sánchez et al., 2009). The nontronite NAu-1, a biotite, a white mica (muscovite), and the Wyoming montmorillonite (SWy-1) were selected to validate their low temperature magnetic properties. The trioctahedral biotite of Bankroft, Ontario, contains 15.8 wt % of Fe under Fe(II) state (Rancourt et al., 1993; Chon et al., 2003). The muscovite reference is dioctahedral and has low iron content (1.4 wt %), assumed to be Fe(III). Montmorillonite SWy-1 is dioctahedral and has also low iron content (3.1 wt %; American Clay Society Standard), assumed to be Fe(III) (e.g. Chipera and Bish, 2001). Contrastingly, dioctahedral nontronite NAu-1 has high iron content (13.2 wt %; Keeling et al., 2000) and is thus the most favorable mineral to perhaps display a specific magnetic behavior. Among carbonates, siderite ($FeCO_3$) is the iron end member. In COx Clay Formation, siderite (<2%) exhibits almost similar chemical compositions, and contains significant amounts of Ca and Mg (in substitution of Fe), and is thus called sideroplesite according to Mozley (1989) (Lerouge et al., 2011, 2012). Siderite is paramagnetic at room temperature, becomes antiferromagnetic when passing through its Néel temperature (~38 K; Frederichs et al., 2003; Kosterov et al., 2006). To ensure that sideroplesite behaves similarly, a sideroplesite sample separated from a concretion observed in Opalinus core sample

from the Benken borehole at depth 559.05 m (northern Switzerland) was analyzed (Mazurek et al., 2009; 2011).

Table A1: List of the minerals used as references, their provenance and their structural formula

Biotite, Silver Crater mine, near Bancroft, Ontario, Canada (Chon et al., 2003)
$(K_{1.96}Na_{a13}Ca_{0.01})(Mg_{3.15}Fe_{2.59}^{2+}Ti_{0.17}Mn_{0.09})(Si_{5.98}Al_{1.92}Ti_{0.10})O_{20}[(OH)_{1.47}F_{1.98}]$
Muscovite (unknown) (EPMA analyses, this study)
$(K_{1.77}Na_{0.19})(Mg_{0.15}Fe_{0.21}^{3+}Mn_{0.01})(Si_{6.13}Al_{5.56}Ti_{0.03})O_{20}\ (OH)_4$
Na-Montmorillonite SWy-1 (Newcastle formation, State of Wyoming, USA) (Copyright © 2003-2012 The Clay Minerals Society)
$(K_{0.05}Na_{0.32}\ Ca_{0.12})(Mg_{0.54}Fe_{0.41}^{3+}Mn_{0.01}\ Al_{3.01}Ti_{0.02})(Si_{7.98}Al_{0.02})O_{20}\ (OH)_4$
Nontronite NAu-2, Uley graphite mine, South Australia (Keeling et al., 2000)
$(M^{+}_{0.97})(Mg_{0.70}Fe_{3.32}Mn_{0.01}\ Al_{0.52}Ti_{0.02})(Si_{7.57}Al_{0.01}Fe_{0.42})O_{20}(OH)_4$
Siderite (Benken borehole, Switzerland)
$(Fe_{0.71}^{2+}Ca_{0.13}Mg_{0.15}Mn_{0.01})CO_3$

1.2 Samples preparation

Samples used as references were not preserved from atmosphere. Biotite and muscovite were prepared from centimeter-sized natural samples. Both were firstly delaminated and each sheet was cleaned with 95 % alcohol under the binocular in order to eliminate visible iron oxy-hydroxides. The samples were finely crushed in an agate mortar and then wedged inside gelatin capsules for magnetic measurements.

Nontronite NAu-1 (Uley graphite mine, South Australia; Keeling et al., 2000) and montmorillonite SWy-1 were purchased from the Clay Source Repository. Montmorillonite was not subjected to any purification process, and may thus contain traces of Fe oxides (e.g. Chipera and Bish, 2001). Contrastingly, two samples of nontronite NAu-1 (NAu-1_(1) and NAu-1_(2)) were purified according to two different protocols described respectively in Gailhanou et al. (2013) and Hadi et al. (2013). According to Gailhanou et al. (2013), the fraction of particle diameter lower than 2 µm of nontronite was separated by centrifugation. Then, the nontronite sample was Ca-saturated in a 1 M $CaCl_2$ solution for 24 h. After washing the solid in deionized water, the absence of chloride ions was checked using the $AgNO_3$ test. The structural formula of NAu-1_(1) is:

$Ca_{0.247}\ K_{\ 0.020}\ (Si_{3.458}\ Al_{0.542})(Mg_{0.066}Fe^{3+}_{1.688}Al_{0.268}Ti_{0.007})O_{10}(OH)_2$

X-Ray diffraction (XRD) analyzes and modeling of ^{57}Fe Mössbauer spectra revealed the presence of 2 wt% of goethite (Gailhanou et al., 2013).

According to Hadi et al. (2013), purification and fractionation of the fraction of particle diameter lower than 2 µm have been carried out by elutriation technique (Claret et al., 2010). The structural formula of Nau-1_(2) is:

$Na_{0.07}\ K_{0.03}\ Ca_{0.29}\ Mg_{0.15}\ (Mg_{0.06}Fe^{3+}_{3.24}Al_{0.74})\ (Si_{6.93}\ Al_{0.97}\ Fe_{0.06})\ O_{20}(OH)_4$

XRD analyze and modeling of ^{57}Fe Mössbauer spectra do not reveal the presence of goethite (Hadi et al., 2013).

1.3 Results

Siderite, biotite, muscovite, and montmorillonite were measured with the sequence A (see methods in this appendix); nontronites with the sequences A and B.

Muscovite and biotite magnetic behaviors are very noisy, as expected for paramagnetic minerals (Figures A1c and A1d).

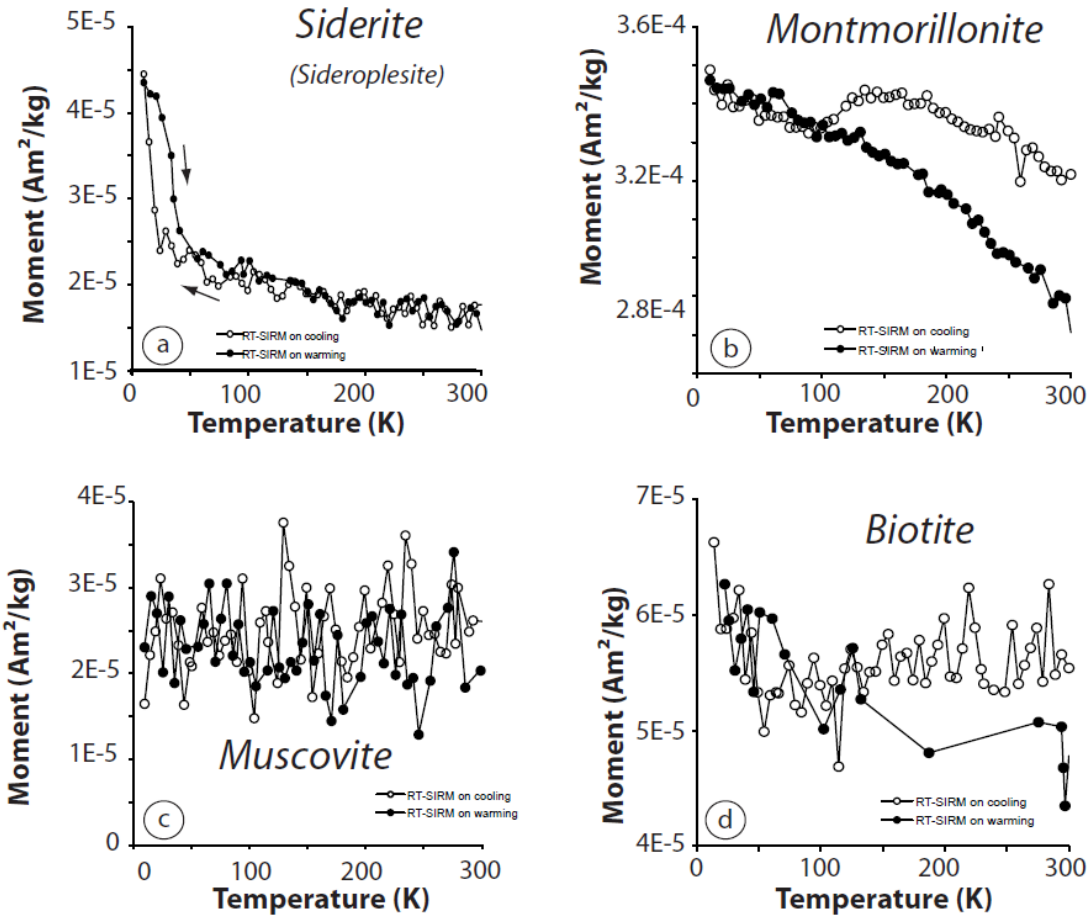

Figure A1: Low temperature magnetic behavior for selected Fe-bearing minerals

SWy-1 montmorillonite displays a particular magnetic behavior at low temperature (Figure A1b). The remanence increases very slightly by 8% from 300 to 10 K. This low percentage could be due to maghemite or goethite. The remanence decreases at 120 K which is unrecovered when warming back to room temperature. This magnetic behavior corresponds to the Verwey transition of magnetite (e.g. Özdemir et al., 2002). Although this mineral was not previously reported to occur in SWy-1 montmorillonite, previous studies had demonstrated the minor presence of other iron oxides (e.g. Chipera and Bish, 2001). A complementary infrared spectrum on SWy-1 montmorillonite reveals a discrete peak at 1386 cm^{-1} corresponding to goethite (Figure A2b). Both magnetic and goethite occur as inclusions in minute amounts in the SWy-1 montmorillonite.

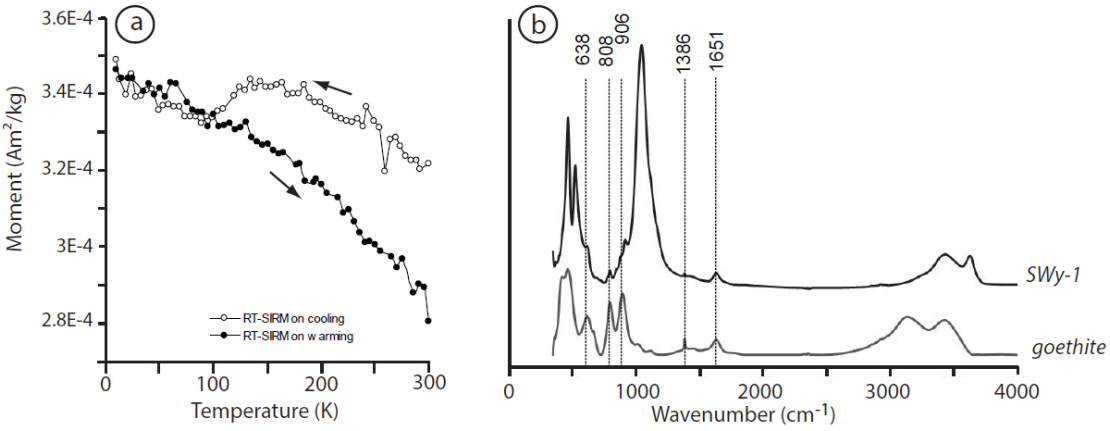

Figure A2: a) Evolution of the RT-SIRM of SWy-1 montmorillonite trough a cooling-warming cycle. Note the 6% increase of the remanence from 300 to 150 K and the Verwey transition of magnetite; b) Infrared spectrum of montmorillonite SWy-1 showing the presence of minute amount of goethite.

When cooling down to 10 K, the remanence of sideroplesite is almost linear down to ~150 K and then increases slowly (Figure A1a). The remarkable feature is the abrupt increase by 2 of the remanence from ~ 40 to 10 K. This magnetic behavior is almost reversible, and might correspond to a change in magnetic state similarly to the siderite specimen analyzed by Frederichs et al. (2003) (not a pure siderite). One has to notice that the measurement is supposed performed under a null magnetic field (< 0.1 μT). In a true null magnetic field, paramagnetic Fe-Mn carbonates are not capable to retain a remanence. The evolution of the remanence observed below ~ 40 K is thus probably due to the presence of the trapped field inside the magnetometer. At low temperature,

the presence of a small magnetic field indeed exacerbates the magnetic transitions of paramagnetic minerals (Aubourg and Pozzi, 2010; Kars et al., 2011). Based on low temperature magnetic measurements, no other magnetic phase is identified in the Benken sideroplesite sample.

The most interesting magnetic behaviors for silicates come from the two studied nontronites.

NAu-1_(1) nontronite is known to contain 2 wt% of goethite (Gailhanou et al., 2013). The remanence of NAu-1_(1) nontronite imparted at room temperature (M1 = $1.78.10^{-3}$ Am^2 kg^{-1}) increases by ~3 times from 300 to 10 K (Figure A3a); that is typical of goethite and confirms previous observations. The presence of goethite is also comforted by a complementary infrared spectrum on bulk nontronite revealing a discrete peak at 1386 cm^{-1} which corresponds to goethite (Figure A3b), and by micro-Raman spectra on a few identified µm-sized brownish particles identified as goethite particles (Figure A3c).

NAu-1_(2) nontronite is not known to contain goethite (Hadi et al., 2013). The remanence imparted at room temperature (M1 = $1.6.10^{-4}$ Am^2 kg^{-1}) is one order of magnitude lower than NAu-1_(1) ($1.78.10^{-3}$ Am^2 kg^{-1}). Remanence increases by ~4 times from 300 to 10 K, also suggesting the presence of goethite in the sample (Figure A4a). The SIRM evolution on cooling-warming cycles is reversible. A very slight change-in-slope occurring at ~270 K may indicate the occurrence of hematite (Figure A4b). By comparison with Nau-1_(2), complementary infrared spectrum of bulk nontronite does not reveal any peak of goethite or hematite, whereas micro-Raman spectra on very rare µm-sized brownish particles allow identifying goethite particles (Figures A4c and A4d).

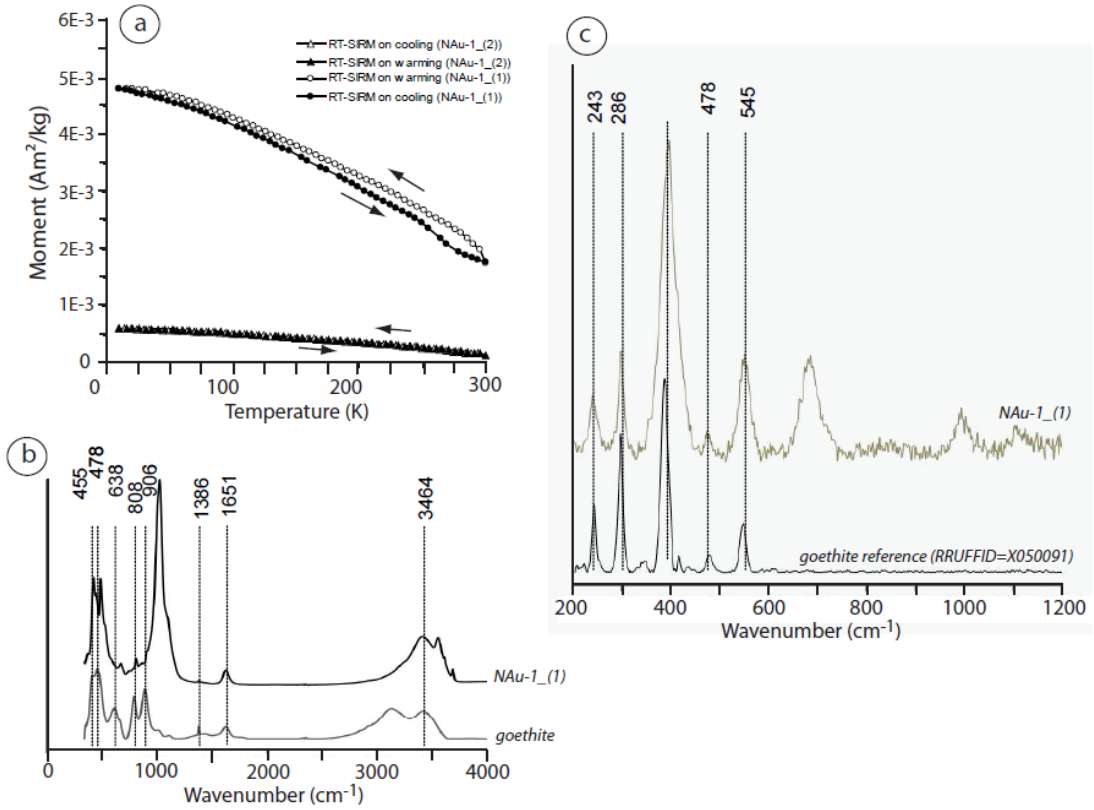

Figure A3: a) Evolution of the RT-SIRM of the nontronite NAu-1_(1) during a cooling-warming cycle compared to the one of NAu-1_(2). Note that NAu-1_(1) is one order of magnitude higher than NAu-1_(2); b) Infrared spectrum of nontronite NAu-1_(1) and goethite; c) Raman spectrum of a µm-sized particle in nontronite NAu-1_(1). The spectrum of a goethite (RRUFFID=X050091) is given for reference.

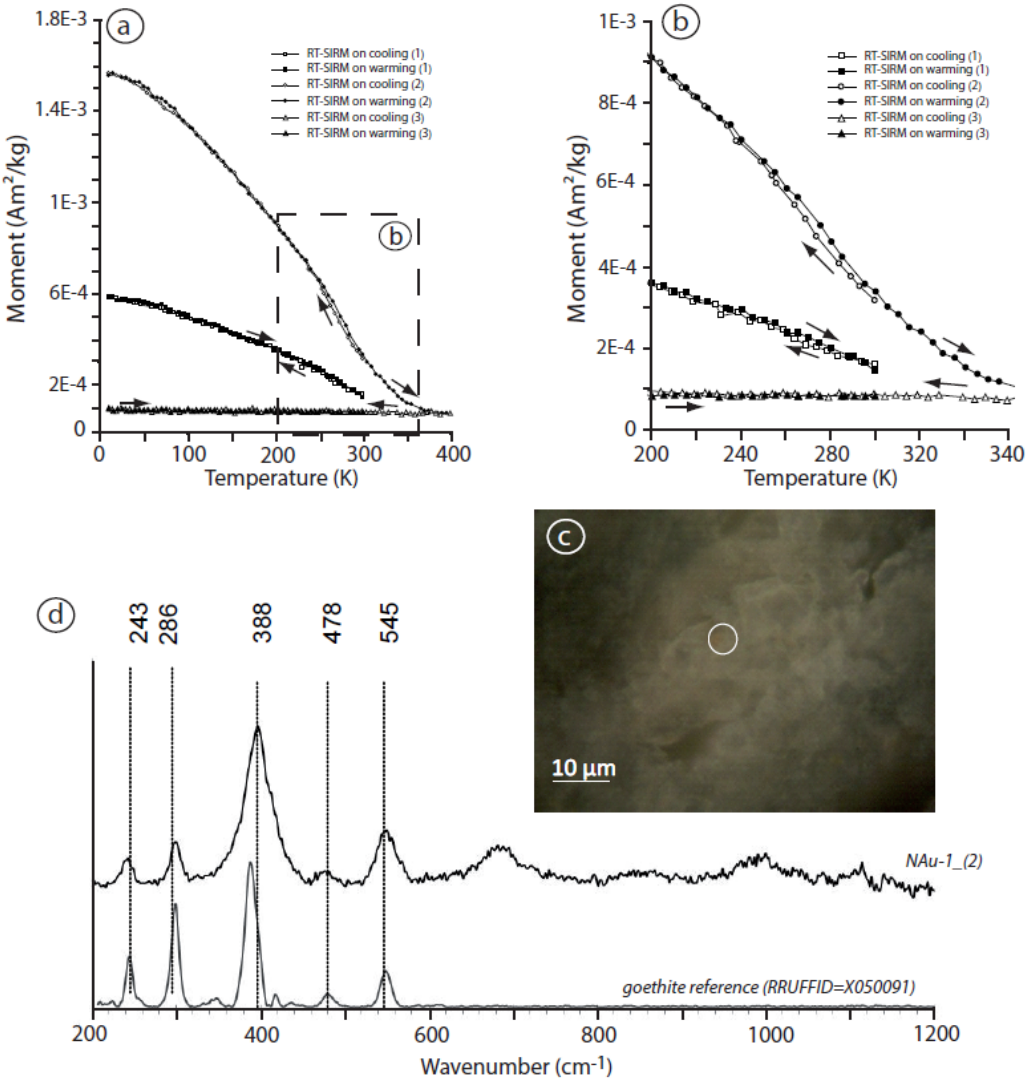

Figure A4: a, b) Evolution of the RT-SIRM on three successive cooling-warming cycles for NAu-1_(2) sample; c) micrograph in reflected light of a µm-size goethite particle on nontronite NAu-1_(2) sample; d) Raman spectrum of a µm-sized particle in NAu-1_(2). The spectrum of a goethite (RRUFFID=X050091) is given for reference.

1.4 Contribition of Fe-bearing minerals

From the above observations, the phyllosilicates that have a low Fe content may not contribute in any significant way to the magnetic signal of the natural bulk claystones. In the COx clays, some phyllosilicates may have however a high Fe content. The most obvious of them is chlorite, which may contain ~20 % Fe (Lerouge et al., 2011). Pure chlorite is very difficult to obtain and it is moreover Fe(II)-bearing mineral. As this study focused on Fe(III)-bearing minerals, nontronite was selected because it is assumed to be the phyllosilicates "Fe-rich end-member". The two analyzed nontronites

show a characteristic magnetic behavior (Figures A3 and A4). This magnetic signal is typical of goethite. Occurrence of goethite in the nontronite specimens is likely due to residual impurities resulting from the extraction process.

Siderite is known to be present in the EST26479 sample in a non-negligible content (~2 %). No characteristic Néel transition is observed at ~40 K in the EST26479 sample, suggesting that siderite, if present, might have its signature hidden by the goethite contribution (Figure A1A).

2. Methods

2.1 Low temperature magnetic measurement

See main text for explanation

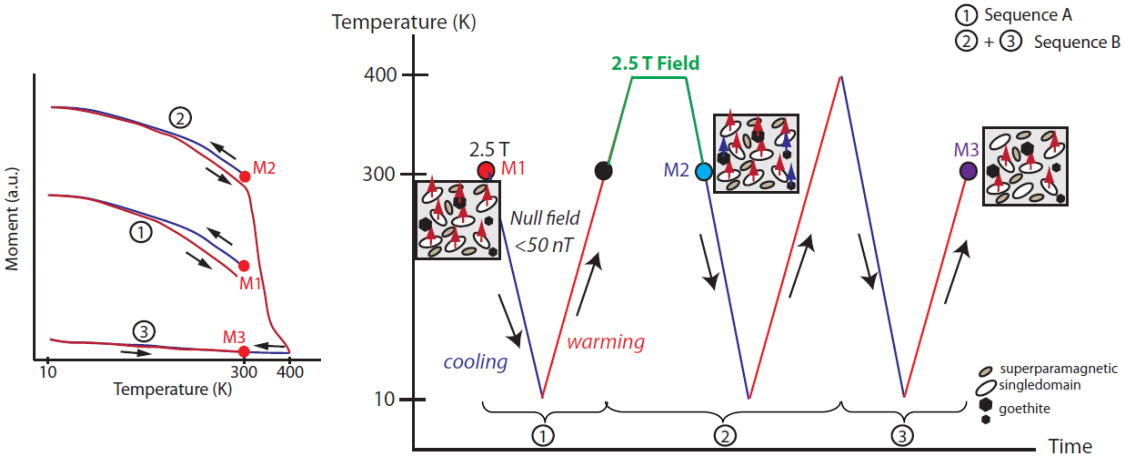

Figure A5: Schematic representation of the MPMS measurement sequences used in this study (at the Institut de Physique du Globe de Paris)

2.2 Infrared spectrometry

Infrared spectra were obtained on a BRUKER Equinox IFS55 spectrometer by transmission through a pellet of a mixture of 150 mg KBr with less than 1 mg of sample. 32 scans were performed for each spectrum from 4000 to 350 cm^{-1}. The spectral resolution is 4 cm^{-1}.

3. Data LT measurements Table A2

Table A2: Remanence values, M1, M2 and M3 for the analyzed samples at low temperature.

Sample	Mass (mg)	M1 (Am^2/kg)	M2 (Am^2/kg)	M3 (Am^2/kg)
Goethite	562	$8.25.10^{-3}$	$2.84.10^{-2}$	$1.22.10^{-3}$
FOR1118 Claystones	247 (fragment preserved)	$1.05.10^{-4}$		
	427 (powder preserved)	$1.52.10^{-4}$	$1.58.10^{-4}$	$1.21.10^{-4}$
	373 (24h air)	$6.77.10^{-5}$		
Organic matter+pyrite extract	394	$1.18.10^{-4}$		
K119	354	$8.72.10^{-5}$		

References cited

Aubourg, C. and J-P. Pozzi, 2010, Toward a new < 250°C pyrrhotite-magnetite geothermometer for claystones, *Earth and Planetary Science Letters*, 294(1-2), 47-57.

Ballet, O. and J.M.D. Coey, 1982, Magnetic properties of sheet silicates; 2:1 layer minerals, *Physics and Chemistry of Minerals*, 8, 218-229.

Chipera, S.J. and D.L. Bish, 2001, Baseline studies of the Clay Minerals Society Source Clays: powder X-ray diffraction analyses, *Clays and Clay Minerals*, 49, 398-409.

Chon, C-M., S.A. Kim and H-S. Moon, 2003, Crystal structures of biotite at high temperatures and of heat-treated biotite using neutron powder diffraction, *Clays and Clay Minerals*, 51(5), 519-528.

Claret, F., C. Lerouge, T. Laurioux, M. Bizi, T. Conte, J.P. Gesthem, G. Wille, T. Sato, E.C. Gaucher, E. Giffaut and C. Tournassat, 2010, Natural iodine in a clay formation: implications for iodine fate in geological disposals, *Geochimica et Cosmochimica Acta*, 74(1), 16-29.

Coey, J.M.D., O. Ballet, A. Moukarika and J.L. Soubeyroux, 1981, Magnetic properties of sheets silicates; 1:1 layer minerals, *Physics and Chemistry of Minerals*, 7, 141-148.

Frederichs, T., T. von Dobeneck, U. Bleil and M.J. Dekkers, 2003, Towards the identification of siderite, rhodochrosite and vivianite in sediments by their low-temperature magnetic properties, *Physics and Chemistry of the Earth,* 28, 669-679.

Gailhanou, H., P. Blanc, J. Rogez, G. Mikaelian, K. Horiuchi, Y. Yamamura, K. Saito, H. Kawaji, F. Warmont, J-M. Grenèche, P. Vieillard, C. Fialips, E. Giffaut and E.C. Gaucher, 2013, Thermodynamic properties of saponite, nontronite, and vermiculite derived from calorimetric measurements, *American Mineralogist*, 98(10), 1834-1847.

Hadi, J., C. Tournassat, I. Ignatiadis, J-M. Grenèche and L. Charlet, 2013, Modelling CEC variations versus structural iron reduction levels in dioctahedral smectite. Existing approaches, new data and model refinement, *Journal of Colloid and Interface Science*, 407, 397-409.

Lerouge, C., S. Grangeon, E.C. Gaucher, C. Tournassat, P. Agrinier, C. Guerrot, D. Widory, C. Fléhoc, G. Wille, C. Ramboz, A. Vincot and S. Buschaert, 2011, Mineralogical and isotopic record of biotic and abiotic diagenesis of the Callovian-Oxfordian clayey formation of Bure (France), *Geochimica et Cosmochimica Acta*, 75(10), 2633-2663.

Lerouge, C., S. Grangeon, C. Fléhoc, S. Buschaert, M. Mazurek, J-M. Matrey and C. Tournassat, 2012, Diagenetic carbonates in clay-rich marine formations, International Meeting "Clays in natural and engineered barriers for radioactive waste confinement", Montpellier.

Kars, M., C. Aubourg, and J-P. Pozzi, 2011, Low temperature magnetic behaviour near 35 K in unmetamorphosed claystones, *Geophysical Journal International*, 186, 1029-1035.

Kosterov, A., T. Frederichs and T. von Dobeneck (2006), Low-temperature magnetic properties of rhodochrosite (MnCO3), *Physics of the Earth and Planetary Interiors*, 154, 234-242.

Keeling, J.L., M.D. Raven and W.P. Gates, 2000, Geology and characterization of two hydrothermal nontronites from weathered metamorphic rocks at the Uley Graphite Mine, South Australia, *Clays and Clay Minerals*, 48(5), 537-548.

Martín-Hernández, F. and A.M. Hirt, 2003, The anisotropy of magnetic susceptibility in biotite, muscovite and chlorite single crystals, *Tectonophysics*, 367(1-2), 13-28.

Mazurek, M., P. Alt-Epping, A. Bath, T. Gimmi and H.N. Waber, 2009, Natural tracer profiles across argillaceous formations: the CLAYTRAC project, OECD/NEA Report 6253, OECD Nuclear Energy Agency, Paris, France.

Mazurek, M., P. Alt-Epping, A. Bath, T. Gimmi, H.N. Waber, S. Buschaert, P. De Cannière, M. De Craen, A. Gautschi, S. Savoye, A. Vinsot, I. Wemaere and L. Wouters, 2011, Natural tracer profiles across argillaceous formations, *Applied Geochemistry*, 26(7), 1035-1064.

Mozley, P.S., 1989, Relation between depositional environment and the elemental composition of early diagenetic siderite, *Geology*, 17(8), 704-706.

Özdemir, O., D. Dunlop and B. Moskowitz, 2002, Changes in remanence, coercivity, and domain state at low temperature in magnetite, *Earth and Planetary Science Letters*, 194, 343-358.

Rancourt, D.J., P. Tume and A.E. Lalonde, 1993, Kinetics of the $(Fe^{2+}+OH^{-})_{mica} \rightarrow (Fe^{3+}+O^{2-})_{mica}$ + H oxidation reaction in bulk single-crystal biotite studied by Mössbauer spectroscopy, *Physics and Chemistry of Minerals*, 20, 276-284.

Rivas-Sánchez, M.L., L.M. Alva-Valdivia, J. Arenas-Alatorre, J. Urrutia-Fucugauchi, M. Perrin, A. Goguitchaichvili, M. Ruiz-Sandoval and M.A. Ramos Molina, 2009, Natural magnetite nanoparticles from an iron-ore deposit: size dependence on magnetic properties, *Earth Planets Space*, 61, 151-160.